Coordination Chemistry Reviews 253 (2009) 2686–2697

Contents lists available at ScienceDirect

Coordination Chemistry Reviews

journal homepage: www.elsevier.com/locate/ccr

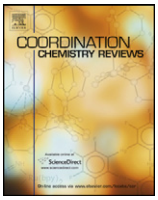

Review

An approach to describing the topology of polynuclear clusters

George E. Kostakis[a], Annie K. Powell[a,b,*]

[a] Institute for Nanotechnology, Forschungszentrum Karlsruhe, Karlsruhe Institute of Technology, Postfach 3640, D-76021 Karlsruhe, Germany
[b] Institut für Anorganische Chemie der Universität Karlsruhe, Karlsruhe Institute of Technology, Engesserstr. 15, D-76131 Karlsruhe, Germany

Contents

ARTICLE INFO

Article history:
Received 31 March 2009
Accepted 9 May 2009
Available online 18 May 2009

Keywords:
Polynuclear clusters
Coordination chemistry
Topology

ABSTRACT

The literature on metal clusters reveals numerous examples of polynuclear clusters made up of ions with open shells displaying interesting structural, chemical and physical properties. For example, such clusters are found in biology and are modeled in bioinorganic, biomimetic chemistry. Another area of current intense research activity looks at open shell clusters, which behave as nanoscale magnetic materials, which on a molecular level are denoted as Single-Molecule Magnets or SMMs. In contrast to most closed shell clusters many of these clusters possess topologies which are difficult to describe in terms of familiar polyhedra. The central idea of this tutorial is to extend the accepted and useful topological description according to Schläfli symbols applied to networks in order to introduce a new and convenient approach to describing the topology of polynuclear clusters.

1. Introduction

As a result of improved synthetic strategies it is now possible to direct synthesis towards the production of various structural cluster motifs of collections of open shell metals. Nevertheless, the so-called serendipitous synthesis of such cluster compounds can also lead to unexpected structures where it is difficult to find a satisfactory description of the core structure. Clusters of particular interest are those with relevance to bioinorganic chemistry and to molecule-based nanoscale magnetic materials, which are generally described as Single-Molecule Magnets or SMMs. Up to now, the largest polynuclear species involving open shell ions structurally characterized is the anionic cluster $[H_xMo_{368}O_{1032}(SO_4)_{48}(H_2O)_{240}]^{48-}$ containing 112 Mo(V) and 256 Mo(IV) centers [1]. In contrast, the largest closed shell compound structurally characterized is $[Ag_{490}S_{188}(S_tC_5H_{11})_{144}]$ [2]. In both

---

* Corresponding author at: Institut für Anorganische Chemie der Universität Karlsruhe, Karlsruhe Institute of Technology, Engesserstr. 15, D-76131 Karlsruhe, Germany. Tel.: +49 721 608 2135; fax: +49 721 608 8142.
E-mail address: powell@aoc.uni-karlsruhe.de (A.K. Powell).

0010-8545/$ – see front matter © 2009 Elsevier B.V. All rights reserved.
doi:10.1016/j.ccr.2009.05.002

these examples closed shell metal ions can be regarded as directing the structural topology to give relatively familiar arrangements identifiable in terms of well-known polyhedral representations. On the other hand, clusters comprising exclusively open shell ions are nearly always less easy to describe. Here the largest aggregate so far identified is Mn_{84} [3], which contains Mn(III) ions (d^4) and the cluster which has highest ground spin state of 83/2 is Mn_{19} [4], which contains Mn(II) and Mn(III) (d^5 and d^4) ions. In terms of bioinorganic chemistry, the most realistic miniature model for loaded ferritin is Fe_{19} comprising Fe(III) (d^5) ions [5] and for the active centers of ferredoxin the Fe_4S_4 clusters variously with Fe(II) and Fe(III) (d^6 and d^5) ions [6].

Up to now the structural description of each such cluster has relied on the visual point-of-view of each author and tends to be a description in terms of various, usually distorted, polyhedra. In recent years, in another field of inorganic/coordination chemistry which deals with the description of coordination polymers and metal–organic frameworks, or MOFs, the complicated polynuclear networks which extend in two or three dimensions can be simplified in terms of “nodes” and “linkers”. These can often be categorized as possessing structures of minerals, such as diamond [7], PtS [8], $CdSO_4$ [9], etc. or else assigned new structural descriptions. In this procedure, normally speaking the metal centers or cluster building units are replaced by “nodes” and the (in)organic ligands are designated as the “linkers”.

In the polynuclear clusters of interest there are heteroatoms, such as N, O, S, which can bridge 2–6 metal centers, often giving rise to complicated structures, and there is no doubt that in this expanding field many new examples, difficult to describe using familiar polyhedra, will be discovered. Bearing this in mind, we propose an approach where we designate each metal center of a cluster as a straightforward “node”. The bridging heteroatoms then play the role of the “linker”. At this stage, it should emphasized that we are not dealing here with the classic “Cotton” definition of a cluster which possesses M–M bonds, but rather are using a description analogous to that developed by O’Keeffe et al. to describe extended MOF structures [10]. Thus, in order to avoid any misunderstanding we stress that in the *decorated* final product there are no metal–metal bonds.

Thus, using the approach adopted by O’Keeffe et al. we can define a cluster in terms of the connectivity of its vertices. Thus, a vertex with connectivity given by N is connected to N neighbors, with M to M and so on. Overall, we give the connectivity in terms of an (N,M,...)-connected cluster. For example, a cluster with some vertices connected to two neighbors and some to three would be designated as a (2,3)-connected cluster. If there is only one type of connectivity (node), the cluster is uninodal, for two it is binodal, for three it is trinodal and so on.

The symbolic representation then uses numbers, first to specify the size of the smallest ring containing a given node. If there is more than one ring of a given size present, this is indicated by a superscript number denoting the number of times such a ring is present. Furthermore, if rings of other sizes containing this node are also present, their sizes and number of occurrences are given by using further numbers according to the same rules and in ascending order within the bracket for the node.

In summary, the description of a cluster is first in terms of the number of types of nodes and their connectivities, which will be N-connected for a uninodal system (with *N* the number of connections) or N,M,...-connected for polynodal systems. The symbolic representation, as for the Schläfli symbol, then follows by finding the smallest ring, which is given the number corresponding to the number of members in the ring along with the number of occurrences of this ring, denoted as a superscript on the first number, followed by counting the same parameters for all other possible rings for a given node-type. This is then, in accordance with the nomenclature used for describing MOFs, the vertex symbol. These vertex symbols are collected together with each individual description given in parentheses. The number of times a given vertex symbol occurs in a cluster is denoted by a subscript outside the parentheses. Thus a 2,3-connected cluster will have two sets of parameters, one for the 2-connected node and one for the 3-connected node, with these parameters giving the information about the rings containing each node in the form of a total or cluster symbol corresponding to: $(\text{vertex symbol for 2-connected node})_{\text{subscript denoting number of occurrences}}(\text{vertex symbol for 3-connected node})_{\text{subscript denoting number of occurrences}}$.

In this case the 2-connected nodes participate in only a 3-membered ring with the symbol being (3) and the two 3-connected nodes participate in two 3-membered rings and one 4-membered ring with the arithmetic representation being $(3^2.4)$. The number that arises after counting all subscripts gives the total number of the nodes in the cluster. In the cases where some nodes are repeated, then this can be simplified. For example, in the latter example there are four nodes; two for each 2- and 3-connected, therefore the total symbol can be assigned as $(3)_2(3^2.4)_2$.

In order to illustrate the method further, the topological and numerical analyses of some fairly simple and some much more complicated polynuclear clusters which have been synthesized and published, and often come from our own work, are discussed here. The two major aims of this tutorial are to provide a new and simple structural description analysis for polynuclear clusters and to emphasize the numerical analysis of them. For this latter aim we are mindful of the fact that the physicists who can help in the description of the physical properties of systems tend to prefer dealing with numbers rather than pictures.

2. Clusters topology (topological representation)

2.1. $[Dy_3(\mu_3\text{-}OH)_2L_3Cl_2(H_2O)_4][Dy_3(\mu_3\text{-}OH)_2L_3Cl(H_2O)_5]Cl_5\cdot 19H_2O$

In 2006, we reported the synthesis, structures and properties of a system of two independent dysprosium triangles which individually show a vanishing magnetic susceptibility at low temperature. This is unprecedented in systems comprising an odd number of unpaired electrons [11] and it was subsequently demonstrated that the system represents the archetype of an Ising spin triangle [12,13]. The crystal structure of $[Dy_3(\mu_3\text{-}OH)_2L_3Cl_2(H_2O)_4][Dy_3(\mu_3\text{-}OH)_2L_3Cl(H_2O)_5]Cl_5\cdot 19H_2O$ (**1**) (HL=*o*-vanillin) consists of two independent triangles of Dy(III) capped by two μ_3-hydroxo centers (Fig. 1). Note that it is immaterial which of the triangles we choose in order to illustrate the approach since both have the same connectivity.

Simplifying the metal core, we can first note that each node (metal) is connected to two others making this a 2-connected structure. The three metals describe an almost isosceles triangle with distances within the ring of Dy(1)–Dy(2) 3.503 Å, Dy(2)–Dy(3) 3.527 Å and Dy(3)–Dy(1) 3.523 Å. In this way, three 2-connected nodes are formed (follow the blue dashed lines in Fig. 1 right) with the vertex symbol of each node being (3) and, as outlined above, since each node is part of a 3-membered ring only once, no superscript is given. Thus the cluster is *uninodal* with a total or cluster symbol (3).

2.2. $[Co_4(\mu_3\text{-}OH)_2(H_2O)_6(ntp)_2]\cdot 2H_2O$

A hydroxyl-bridged tetranuclear cluster $[Co_4(\mu_3\text{-}OH)_2(H_2O)_6(ntp)_2]\cdot 2H_2O$ (**2**) is formed in the reaction of $CoCl_2\cdot 6H_2O$ and nitrilotripropionic acid ($H_3ntp{=}N(CH_2CH_2COOH)_3$) in the presence of KOH. The Co(II) ions are oxygen bridged and exhibit a defect dicubane-like core with two missing vertices (Fig. 2) [14].

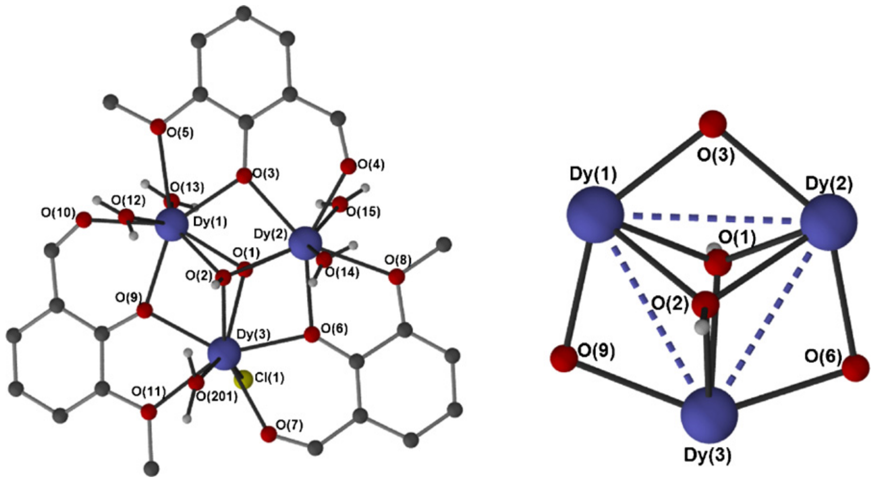

Fig. 1. Structure of the triangular unit in **1** with numbering scheme (left) and the simplified core (right). Color scheme: blue (Dy(III)), red (O), green (Cl), dark gray (C), and white (H). (For interpretation of the references to color in this figure legend, the reader is referred to the web version of the article.)

Magnetic studies reveal competing antiferromagnetic and ferromagnetic interactions between the four Co(II) ions in **2**.

Simplifying the metal–oxygen core, two 2-connected, Co(1) and Co(1′), and two 3-connected, Co(2) and Co(2′), nodes are formed (follow the blue dashed lines in Fig. 2 right). Each of Co(1) and Co(1′) is connected to Co(2) and Co(2′) and these two 2-connected nodes participate in one 3-membered ring each giving the vertex symbol (3). The distances in the ring are Co(1)–Co(2) 3.2026(5) Å, Co(1)–Co(2′) 3.1884(5) Å and Co(2)–Co(2′) 3.1342(7) Å. Each of Co(2) and Co(2′) is connected to Co(1) and Co(1′) and these two 3-connected nodes participate in two 3-membered rings and one 4-membered ring to give the vertex symbol (3^2.4). Therefore, the cluster can be described as a binodal (2,3) and the cluster symbol is (3)(3^2.4).

2.3. $[Fe_4(\mu\text{-}O)(\mu\text{-}OH)_3(5\text{-}Ph\text{-}hxta)_2]^{3-}$

A formal condensation of two dinuclear building blocks [(5-Ph-hxta)$Fe_2(OH)(H_2O)_2$] gives rise to a slightly distorted tetrahedral tetranuclear aggregate corresponding to [(5-Ph-hxta)$_2$$Fe_4(\mu\text{-}O)(\mu\text{-}OH)_3]^{3-}$ (**3**) [15]. The fact that there are three bridging hydroxides and only one bridging oxide means that the core structure is asymmetric. However, using our method, the topology is relatively easy to describe.

Following the blue dashed lines in Fig. 3 (lower) it can be seen that each node in the tetrahedral arrangement is 3-connected and furthermore that each node is part of three 3-membered rings. Take for example the node for Fe(1) which is involved in a 3-membered rings made up from Fe(1)–Fe(2)–Fe(3); one from Fe(1)–Fe(2)–Fe(4) and one from Fe(1)–Fe(3)–Fe(4) to give the vertex symbol (3.3.3). Overall, the tetranuclear aggregate can be described as *uninodal* with a cluster symbol (3^3). A similar arithmetical description, i.e.. the symbol will come out as (3^3), applies to a tetranuclear aggregate possessing a cubane arrangement. Such cubanes compound can be found in a recently reported octadecanuclear heterometallic aggregate $[Ni_{12}Mn_6(bdoa)_6(O_2CMe)_{12}(\mu_3\text{-}OMe)_{12}(MeOH)_{12}]\cdot 21MeOH$ (**4**) (bdoa = benzene-1,2-dioxyacetate) [16], where the cubane structure $[Ni_4(O_2CMe)_4(OMe)_4(MeOH)_4]$ can be recognized. Following the blue dashed lines in Fig. 4 (right) it can be seen that each node in the cubane arrangement is 3-connected and furthermore that each node is part of three 3-membered rings, as previously described. Overall, the tetranuclear aggregate can be described again as *uninodal* with a cluster symbol (3^3).

2.4. $[CaMn(III)_3Mn(II)(\mu_4\text{-}O)L_3Cl_2(O_2CMe)_{1.2}(H_2O)_{1.5}(MeOH)_{0.3}]Cl_{0.8}\cdot 5MeOH$

In 2006, we published a series of compounds which can be of assistance in elucidating the arrangement of metals in the oxygen evolving center (OEC) of photosystem II (PSII) [17]. The central core of the compound $[CaMn(III)_3Mn(II)(\mu_4\text{-}O)L_3Cl_2(O_2CMe)_{1.2}(H_2O)_{1.5}(MeOH)_{0.3}]Cl_{0.8}\cdot 5MeOH$ (**5**) consists of three Mn(III) centers Mn(1)–Mn(2)–Mn(3), each of which is chelated by a tridentate Schiff base ligand L via the deprotonated phenol and propanol oxygens and the imino nitrogen (Fig. 5). These are linked through an oxo ligand O(1), such that the mean planes of the ligands are approximately perpendicular to the planar Mn_3O moiety. Two monodentate ligands, (μ-Cl) and a bidentate acetate provide further bridges between these three Mn(III) centers to give

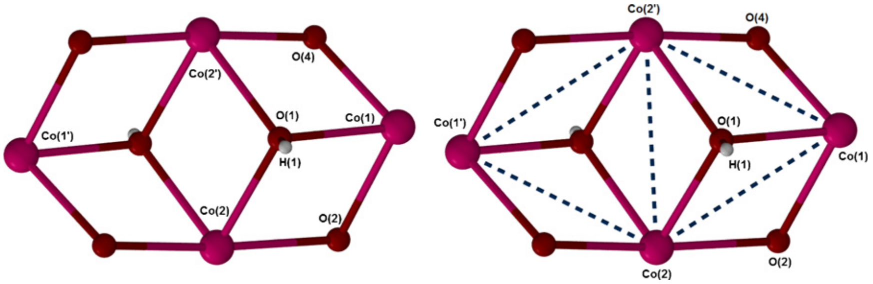

Fig. 2. Molecular structure of the core of $Co_4(OH)_2$ in **2** (left) and its simplified structure (blue dashed lines, right). (For interpretation of the references to color in this figure legend, the reader is referred to the web version of the article.)

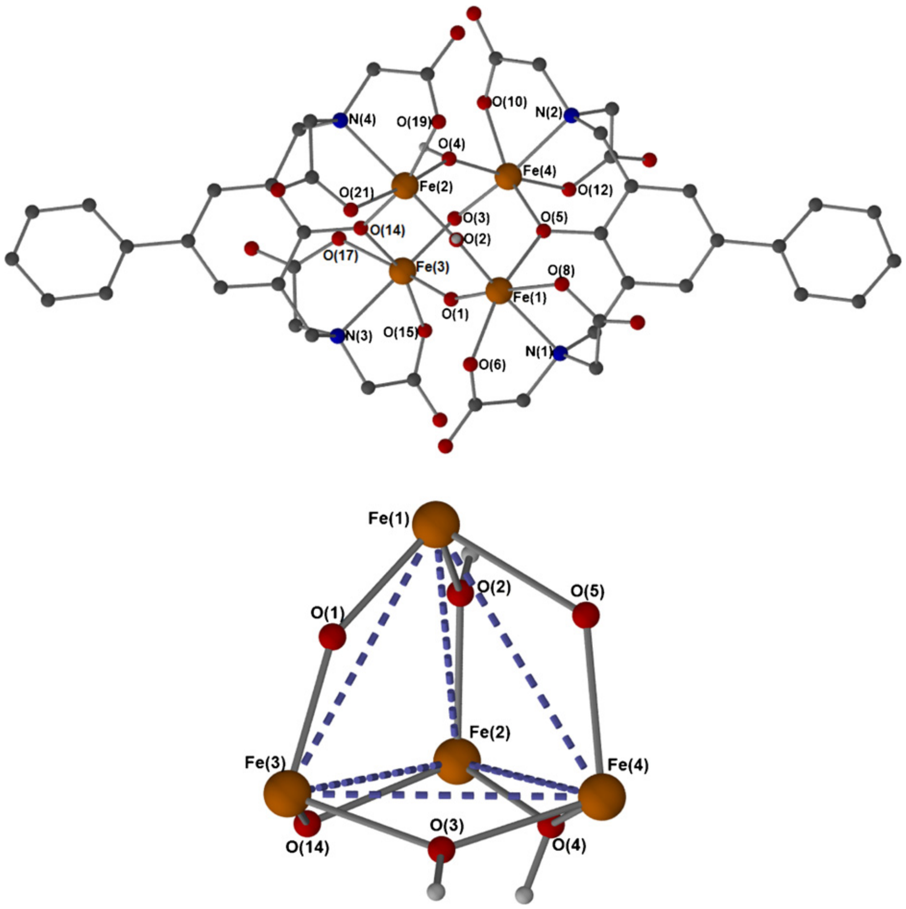

Fig. 3. The molecular structure of **3** (upper) and its simplified core (lower).

an isosceles Mn_3O triangle with two shorter Mn···Mn distances and one longer one. Two deprotonated phenol and one deprotonated propanol oxygens bridge to Mn(4) with a terminal chloride completing the coordination sphere. Conversely, two deprotonated propanol and one deprotonated phenol oxygens bridge to the Ca(II) cation Ca(1), which is further ligated by the central oxo ligand, a water and a disordered mixed monodentate ligand. Magnetic studies reveal the presence of dominating antiferromagnetic interaction between Mn spins giving rise to an $S = 1/2$ ground spin state, which, in conjunction with the composition and core structure makes the system one of the most realistic models for one of the suggested arrangements for the S_0 Kok state in PSII.

Simplifying the core of **5**, a trigonal bipyramidal polyhedron is formed. Ca(1) and Mn(4) are at the apices of the polyhedron, while Mn(1), Mn(2) and Mn(3) form the equatorial plane. Ca(1) and Mn(4) are connected to Mn(1), Mn(2) and Mn(3), forming two 3-connected nodes and three 3-membered rings, while Mn(1), Mn(2) and Mn(3), can be consider as 4-connected nodes with vertex symbol $(3.3.3.3.3.4_2)$. In this way, a binodal (3,4) cluster is formed with total symbol $(3^3)_2(3^5.4)_3$.

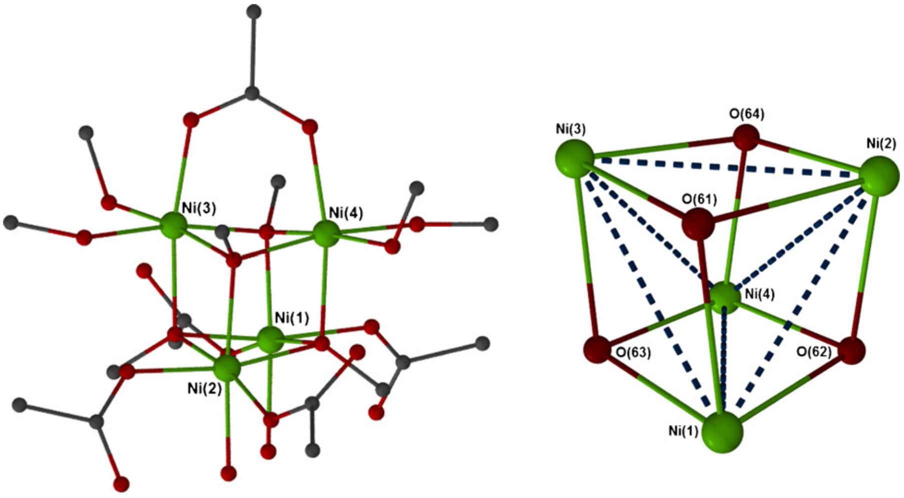

Fig. 4. The self-assembled $\{Ni_4(\mu_3\text{-}OMe)_4\}$ cubane unit (left) and its simplified core (right).

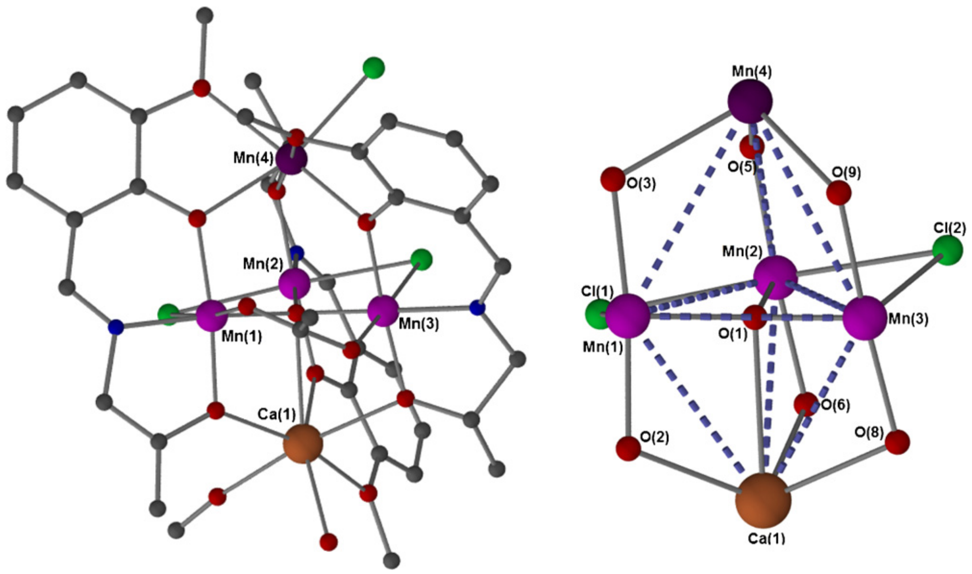

Fig. 5. The molecular structure of **5** (Mn(III)) pink, (Mn(II)) mauve, (Ca) light brown, (O) red, (C) black, (N) blue, (Cl) pale green (left). The simplified structure core of **5** (blue lines, right). (For interpretation of the references to color in this figure legend, the reader is referred to the web version of the article.)

Interestingly, if we compare this description with what has been proposed for the arrangement in the core from the various protein structure determinations and EXAFS studies [17] the total symbol comes out the same, which is the result of the method distinguishing positions, but not the identity of the metal at the node.

2.5. $[Fe(III)_7(\mu_3\text{-}O)_3(teaH)_3(\mu\text{-}O_2CCMe_3)_6(\eta^1\text{-}O_2CCMe_3)_3(H_2O)_3]$

Isostructural heptanuclear Fe(III) compounds displaying a three-blade propeller topology with the central Fe atom representing the axle or axis of the propeller were reported in 2007 [18]. This motif (Fig. 6) is magnetically interesting because it corresponds to the theoretical model of a frustrated Heisenberg star, which is one of the very few solvable models in the area of frustrated quantum-spin systems. Magnetic studies carried on compound $Fe(III)_7(\mu_3\text{-}O)_3(teaH)_3(\mu\text{-}O_2CCMe_3)_6(\eta^1\text{-}O_2CCMe_3)_3(H_2O)_3]$ (**6**) established unequivocally an $S = 5/2$ ground spin state, consistent with overall antiferromagnetic interactions between the constituent Fe(III) ions.

Simplifying the core, the peripheral Fe atoms form two 3-membered rings and one 4-membered ring. This can be seen, for example, taking Fe(2) (follow the dashed blue lines in Fig. 7) which forms 3-membered rings corresponding to Fe(2)–Fe(1)–Fe(3) and Fe(2)–Fe(1)–Fe(3′) and a 4-membered ring corresponding to Fe(2)–Fe(3)–Fe(1)–Fe(3′). The central Fe atom is connected to all the peripheral Fe atoms, and the vertex symbol of the node is $(3.3.3.3.3.3.4.4.4.4.4.4.5_2.5_2.5_2)$ (follow the blue dashed lines in Fig. 6). The three-blade propeller-like cluster can thus be considered as binodal (3,6) with total symbol $(3^2.4)_6(3^6.4^6.5^3)$.

2.6. $[Ni_{12}Mn_6(bdoa)_6(O_2CMe)_{12}(\mu_3\text{-}OMe)_{12}(MeOH)_{12}]\cdot 21MeOH$

As mentioned before in Section 2.3, an octadecanuclear heterometallic aggregate $[Ni_{12}Mn_6(bdoa)_6(O_2CMe)_{12}(\mu_3\text{-}OMe)_{12}(MeOH)_{12}]\cdot 21MeOH$ (**4**) (Fig. 7) was reported [16]. Overall, the octadecanuclear heterometallic aggregate **4** can be described in terms of a trigonal-prismatic framework that corresponds to a central $\{Mn(II)_6(bdoa)_6(\mu\text{-}O_2CMe)_3\}$ core decorated by three self-assembled $\{Ni_4(\mu_3\text{-}OMe)_4\}$ cubane units (Fig. 4). The structure is built up round the central, slightly twisted, trigonal-prismatic $\{Mn_6(bdoa)_6(\mu\text{-}O_2CMe)_3\}$ core, where the triangular faces correspond to two trinuclear units in which each Mn(bdoa) center is bridged, through an outer, non-chelating $bdoa^{2-}$ carboxylate oxygen atom, to the next manganese atom in a cyclic fashion. The resulting $\{Mn_3(bdoa)_3\}$ triangles are linked by three *anti-anti*-bridging acetate ligands to form the prism, which has an idealized D3 (32) molecular symmetry (Fig. 7).

Simplifying the heterometallic core of **4**, all the Mn in the Mn_6 core are equivalent to 4-connected nodes with vertex symbol $(3.4^3.6^2)$. This can be illustrated using Mn(1) as a starting point. It is part of the 3-membered ring Mn(1)–Mn(3)–Mn(5), giving the vertex symbol (3) and then is part of the three 4-membered rings defined by Mn(1)–Ni(1)–Ni(2)–Mn(2), Mn(1)–Mn(5)–Mn(6)–Mn(2) and Mn(1)–Mn(3)–Mn(4)–Mn(2) to give the vertex symbol (4^3). Finally Mn(1) is part of two 6-membered rings defined by Mn(1)–Mn(2)–Mn(6)–Mn(5)–Mn(3)–Mn(4) and Mn(1)–Ni(1)–Ni(4)–Ni(3)–Ni(2)–Mn(2), giving the vertex symbol (6^2) and leading to an overall vertex symbol for this node of $(3.4^3.6^2)$.

Within the Ni cubane, there are two distinct Ni nodes, first the 4-connected nodes that bridge the trigonal-prismatic $\{Mn_6(bdoa)_6(\mu\text{-}O_2CMe)_3\}$ core and the $[Ni_4(O_2CMe)_4(OMe)_4(MeOH)_4]$ cubane units corresponding to the pairs Ni(1), Ni(2); Ni(5), Ni(6) and Ni(9), Ni(10) with vertex symbol $(3^3.4.5^2)$. This can be illustrated taking Ni(1) as an example. Ni(1) is part of three 3-membered rings defined by Ni(1)–Ni(2)–Ni(3), Ni(1)–Ni(2)–Ni(4) and Ni(1)–Ni(3)–Ni(4) which leads to the (3^3) part of the vertex symbol. Ni(1) is also part of one 4-membered ring defined by Ni(1)–Ni(2)–Ni(3)–Ni(4) leading to the vertex symbol (4). Finally for this node, Ni(1) takes part in two 5-membered rings defined by Ni(1)–Mn(1)–Mn(2)–Ni(2)–Ni(3) and Ni(1)–Mn(1)–Mn(2)–Ni(2)–Ni(4) to give the vertex symbol (5^2). Thus for this node the overall vertex symbol is $(3^3.4.5^2)$ and since there are six such vertices the cluster symbol will have the contribution as $(3^3.4.5^2)_6$. Second, there are the 3-connected nodes which occur in pairs on the periphery of the cluster and correspond to Ni(3), Ni(4); Ni(7) Ni(8); Ni(11), Ni(12) and which participate in the cubane unit having the vertex symbol (3.3.3) as already explained before in Section 2.3 for tetrahedral arrangements of metal ions, giving the overall vertex symbol for six such centers as $(3^3)_6$. It is worth pointing out here that the vertex connectivity for tetrahedral arrangements of metal ions will preserve the (3^3) vertex description within the overall vertex symbol, as is clearly

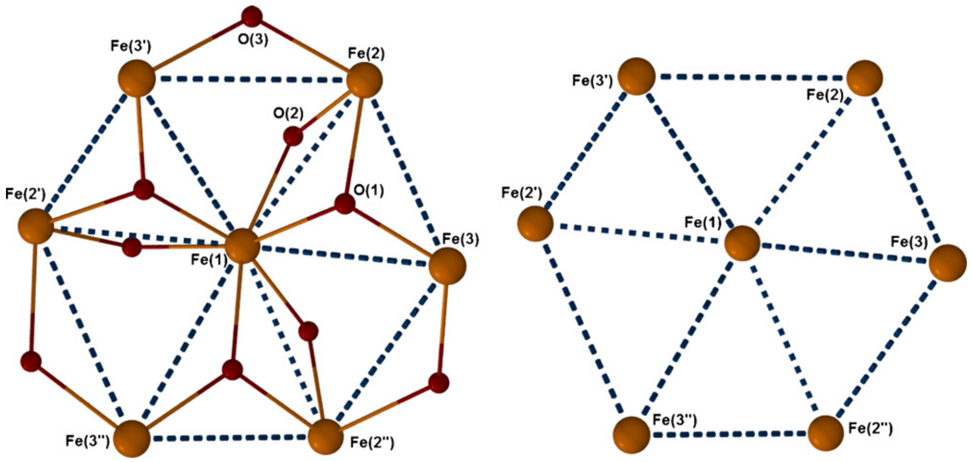

Fig. 6. The core in **6** (left) and its simplified structure (blue lines, right). (For interpretation of the references to color in this figure legend, the reader is referred to the web version of the article.)

the case here for both types of Ni within the cubane unit. Overall, the whole octadecanuclear aggregate can be described as a trinodal cluster with cluster symbol $(3.4^3.6^2)_6(3^3.4.5^2)_6(3^3)_6$.

2.7. [$Mn_{12}O_2(OMe)_2(thme)_4(OAc)_{10}(H_2O)_4$]·2MeOH

The reaction of $Mn(OAc)_2$, 1,1,1-tris(hydroxymethyl)-methane (H_3thme), and triethylamine in methanol leads to the formation of [$Mn_{12}O_2(OMe)_2(thme)_4(OAc)_{10}(H_2O)_4$]·2MeOH (**7**). The [$Mn(III)_4Mn(II)_8$] (Fig. 8) core consists of a central [$Mn(III)_4O_6$] rhombus sandwiched by two [$Mn(II)_4O_7$] fragments. Frequency-dependent ac susceptibility and hysteresis loops in the magnetization indicate single-molecule magnet behavior with a pure quantum-tunneling regime of relaxation below 0.2 K [19].

The central Mn(1) can be replaced by a 8-connected node, with a vertex symbol $(3.3.3.3.3.3.3.3.3.3.3.3.3.3.3.4.4.4.4.4.4_2.4_2.4_2.4_2.4_3.4_3.4_3.5_5)$ while Mn(2) and Mn(3) define two different 6-connected node with vertex symbol $(3.3.3.3.3.3.3.3.3.4.4.4_2.4_2.4_3.5_3)$ and $(3.3.3.3.3.3.3.3.3.3.4.4.4_2.4_3.4_3)$, respectively. Mn(5) and Mn(6) are defined 5-connected nodes with similar connectivity. Their vertex symbol is $(3.3.3.3.3.3.3.4.4_2.4_3)$. Finally Mn(4) defines a 3-connected node and participates in three 3-membered rings. Overall, the cluster can be considered as a six-nodal (3,5,6,8) system with total symbol corresponding to $(3^{10}.4^5)_2(3^{15}.4^{12}.5)_2(3^3)_2(3^7.4^3)_4(3^9.4^5.5)_2$.

2.8. [$Fe(III)_5Ln_8(\mu_3\text{-}OH)_{12}(N\text{-}Bu\text{-}dea)_4(piv)_{12}(NO_3)_4(OAc)_4$]$^-$[$H_3L$]$^+$·x solvent

In recent years we have established a successful synthetic strategy for the construction of Single-Molecule Magnets, SMMs, by combining 3d and 4f metal centers. The coordination sphere of the latter is variable; the most common coordination numbers of the lanthanides are 7, 8 or 9, which means that the shape of the polynuclear cluster can be very complicated. A series of isostructural tridecanuclear mixed-metal [$Fe(III)_5Ln_8(\mu_3\text{-}OH)_{12}$(N-Bu-dea)$_4(piv)_{12}(NO_3)_4(OAc)_4$]$^-$[$H_3L$]$^+$·x solvent (**8**) (Ln = Pr, Nd, Gd) aggregates were reported [20]. The magnetic properties suggest a ferrimagnetic arrangement in the Pr and Nd analogues, whereas for the Gd analogue ferromagnetic interactions are dominant leading to a large spin ground state. The core of the centrosymmetric tridecanuclear cluster can be viewed as consisting of two distorted inner heterometallic [$FeGd_3(\mu_3\text{-}OH)_4$]$^{8+}$ cubane units sharing a common vertex Fe(1), flanked by four edge-sharing heterometallic [$FeGd_2(OH)_4$]$^{5+}$ defect cubane units (Fig. 9).

Simplifying the tridecanuclear metal–oxygen core, Fe(1) is a 6-connected node with a vertex symbol $(3.3.3.3.3.3.4.4.5.5.5.5.5_2.5_2.6_2)$, while both Fe(2) and Fe(3) are 2-connected nodes with vertex symbol (3). Gd(1) is a 3-connected node with a vertex symbol (3.3.3), Gd(2) and Gd(3) are 5-connected nodes with vertex symbol (3.3.3.3.4.5.5.5.6.6) and finally Gd(4) is a

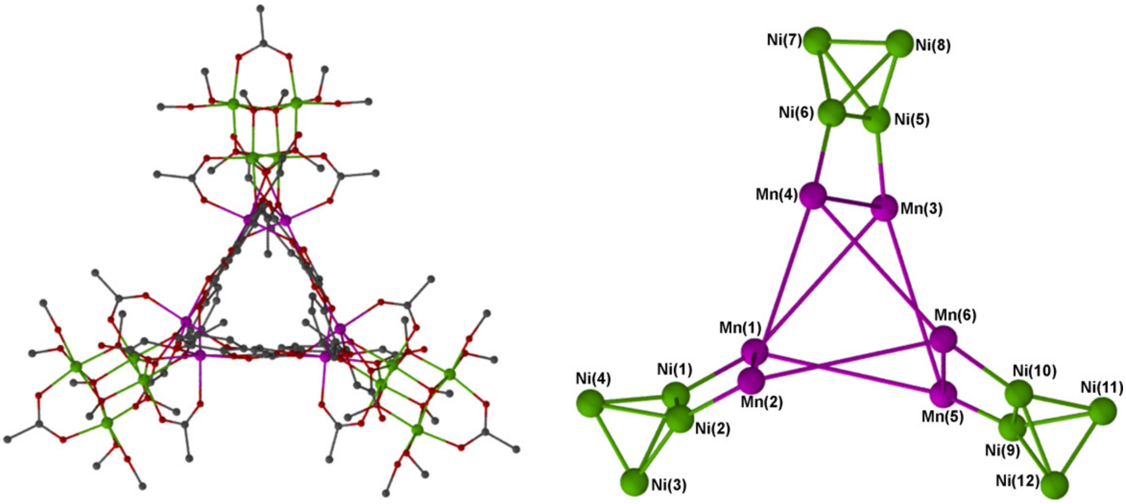

Fig. 7. Molecular structure of the core in **4** (left) and its simplified structure (right). Color scheme: light green (Ni), pink (Mn), red (O) grey (C).

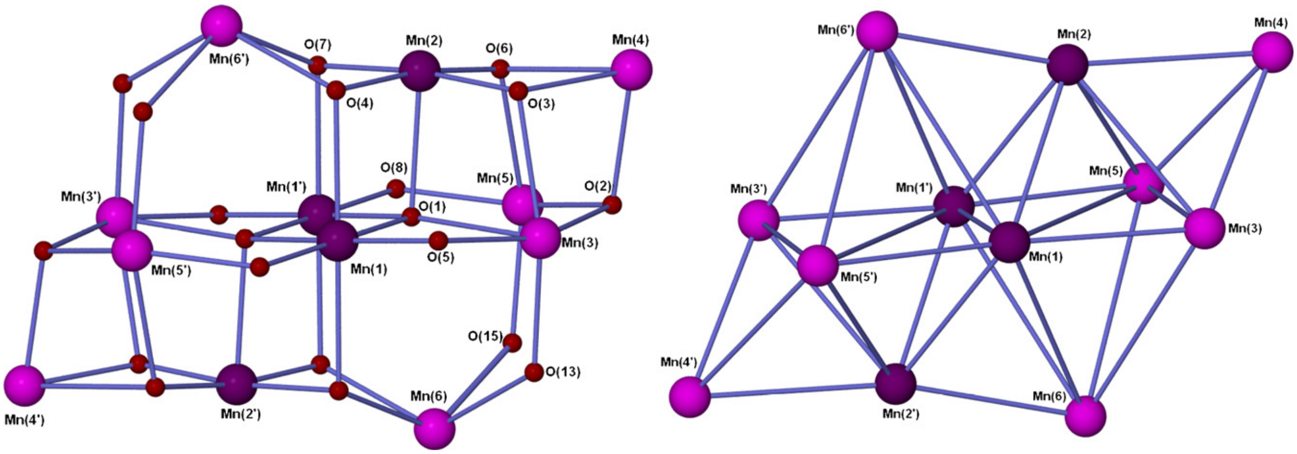

Fig. 8. The Mn–O core in **7** (left) and its simplified structure (blue lines, right). Color code: (Mn(III)) mauve; (Mn(II)) pink. (For interpretation of the references to color in this figure legend, the reader is referred to the web version of the article.)

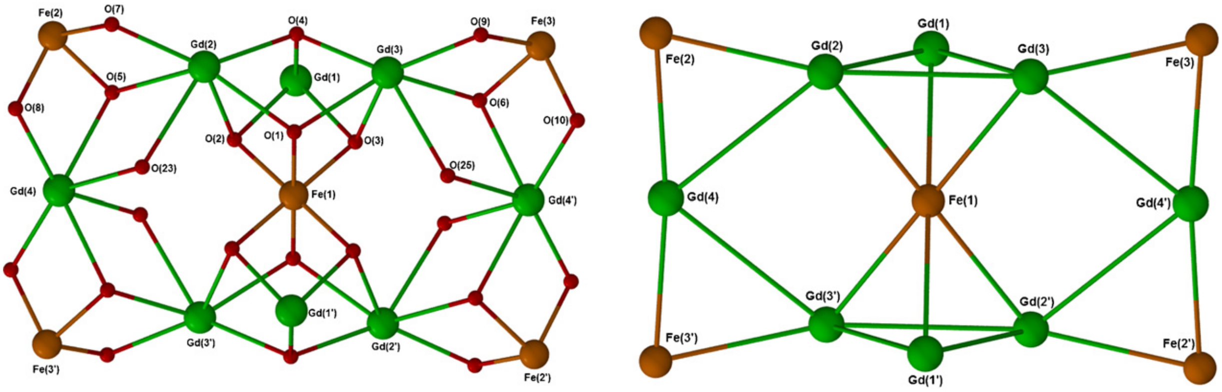

Fig. 9. A view of the metal–oxygen core of $[Fe(III)_5Gd_8(\mu_3\text{-}OH)_{12}(L)_4(piv)_{12}(NO_3)_4(OAc)_4]$ in **8** (left) and its simplified structure (right).

4-connected node and vertex symbol (3.3.4.6.5.5). The cluster can be consider as five-nodal (2,3,4,5,6) and the total symbol is $(3^2.4.5^2.6)_2(3^3)_2(3^4.4.5^3.6^2)_4(3^6.4^2.5^6.6)(3)_4$.

2.9. $[Mn(III)_9Mn(II)_2Gd_2(O)_8(OH)_2(piv)_{10.6}(fca)_{6.4}(NO_3)_2(H_2O)]\cdot 13CH_3CN\cdot H_2O$

Having in mind the anisotropy which arises from Mn(III) and its usefulness in the construction of SMMs, we looked at mixing the high spin of the virtually isotropic Gd(III) ion with Mn(III) and reported the synthesis and properties of the $Mn_{11}Gd_2$, cluster displaying SMM properties, $[Mn^{III}{}_9Mn^{II}{}_2Gd_2(O)_8(OH)_2(piv)_{10.6}(fca)_{6.4}(NO_3)_2(H_2O)]\cdot 13CH_3CN\cdot H_2O$ (**9**) [21]. The core of the $Mn_{11}Gd_2$ aggregate can be described as bell-shaped. The Mn(III) and Mn(II) centers form the shell of the bell, with Mn(9) at the apex, Mn(5), Mn(8), Mn(10), and Mn(11) at the shoulder of the bell, and the remaining six Mn(III) centers forming the rim of the bell. The two Gd centers can be thought of as forming the bell's clapper, and since the Gd···Gd vector is inclined with respect to the axis of the bell; this gives the impression that the bell is ringing (Fig. 10).

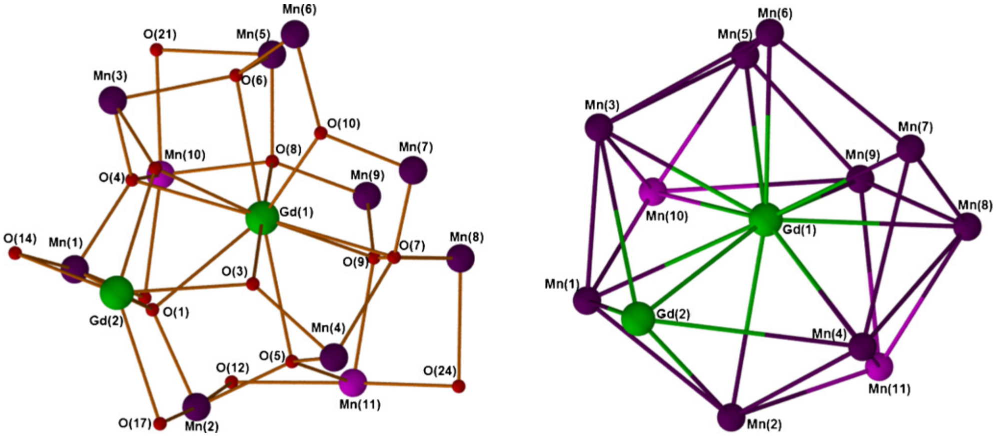

Fig. 10. A view of the metal–oxygen core in **9** (left) and its simplified structure (right).

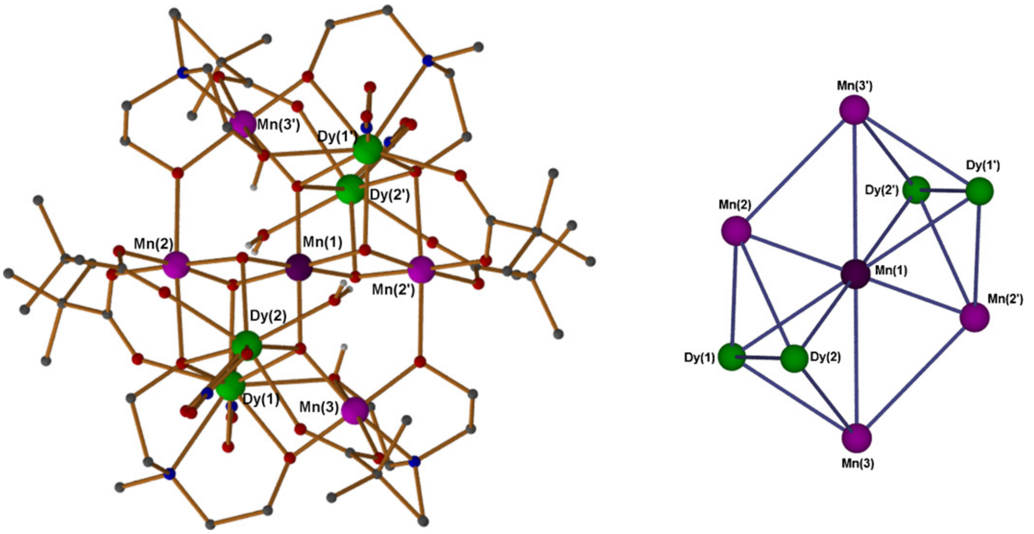

Fig. 11. The molecular structure of **10** (left) and its simplified version (right). Color scheme pink (Mn^{II}), mauve (Mn^{III}), light green (Gd), red (O), grey (C), white (H).

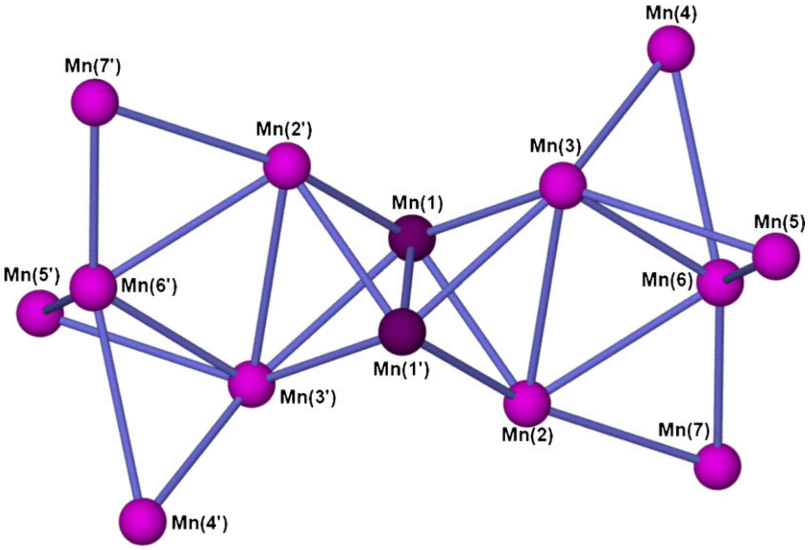

Fig. 12. Simplified structure of compound **11**. Color code: (Mn(III)) mauve; (Mn(II)) pink. (For interpretation of the references to color in this figure legend, the reader is referred to the web version of the article.)

Simplifying the core, Mn(1), Mn(2), Mn(5), Mn(8), Mn(10) and Mn(11) are 5-connected nodes with vertex symbol ($3.3.3.3.3.3.3.4.4_2.4_2$) while Mn(3) and Mn(4) are 6-connected nodes with vertex symbol ($3.3.3.3.3.3.3.3.3.4.4.4.4_2.4_2.4_2$) and Mn(6) and Mn(7) are 4-connected nodes with vertex symbol (3.3.3.4.3.4). Finally Mn(9) is 5-connected node with vertex symbol (3.3.3.3.3.3.4.4.4.4). Gd(1) is a 12-connected node with the short vertex symbol being ($3^{24}.4^{31}.5^{11}$) while Gd(2) is a simple 5-connected node with vertex symbol ($3.3.3.3.3.3.3.4.4_2.4_2$). Therefore, the cluster can be considered as five-nodal with 4,5,6- and 12-connected nodes and total symbol ($3^{24}.4^{31}.5^{11}$)($3^4.4^2$)$_2$($3^6.4^4$)($3^7.4^3$)$_7$($3^9.4^6$)$_2$.

2.10. *[$Mn_5Ln_4(O)_6(mdea)_2(mdeaH)_2(Piv)_6(NO_3)_4(H_2O)_2$]·2MeCN*

Recently, we have presented [$Mn_5Ln_4(O)_6(mdea)_2(mdeaH)_2(Piv)_6(NO_3)_4(H_2O)_2$]·2MeCN, a new family of high-nuclearity 3d–4f compounds representing the first *N*-methyldiethanolamine-based Mn–Ln heterometallic complexes [22]. All these compounds show single-molecule magnet behavior that is tuned by the choice of the lanthanide ion and, in the case of the Dy analogue (**10**), the highest energy barrier to spin inversion reported to date for a heterometallic

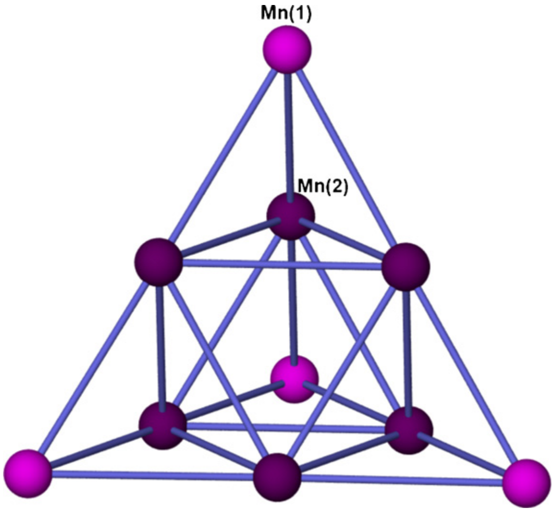

Fig. 13. The simplified structure of **12**. Color code: (Mn(III)) mauve; (Mn(II)) pink. (For interpretation of the references to color in this figure legend, the reader is referred to the web version of the article.)

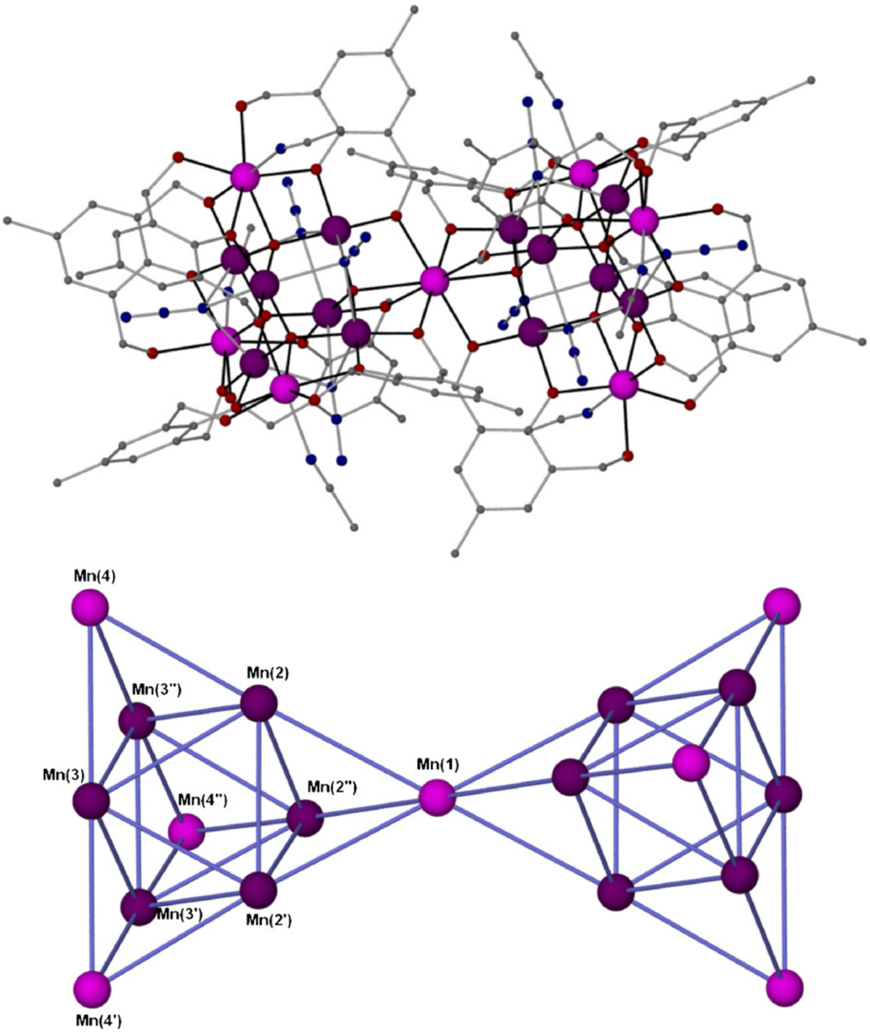

Fig. 14. The molecular structure of **13** (upper) and its simplified version (lower). Color code: (Mn(III)) mauve; (Mn(II)) pink. (For interpretation of the references to color in this figure legend, the reader is referred to the web version of the article.)

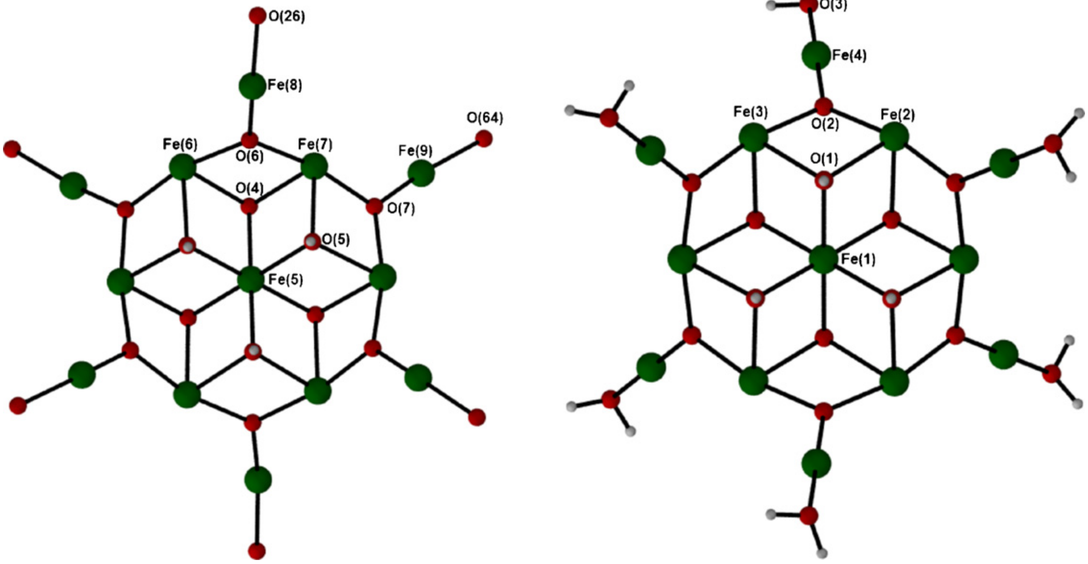

Fig. 15. The molecular core structure of cluster A (left) and cluster B (right) found in **14**.

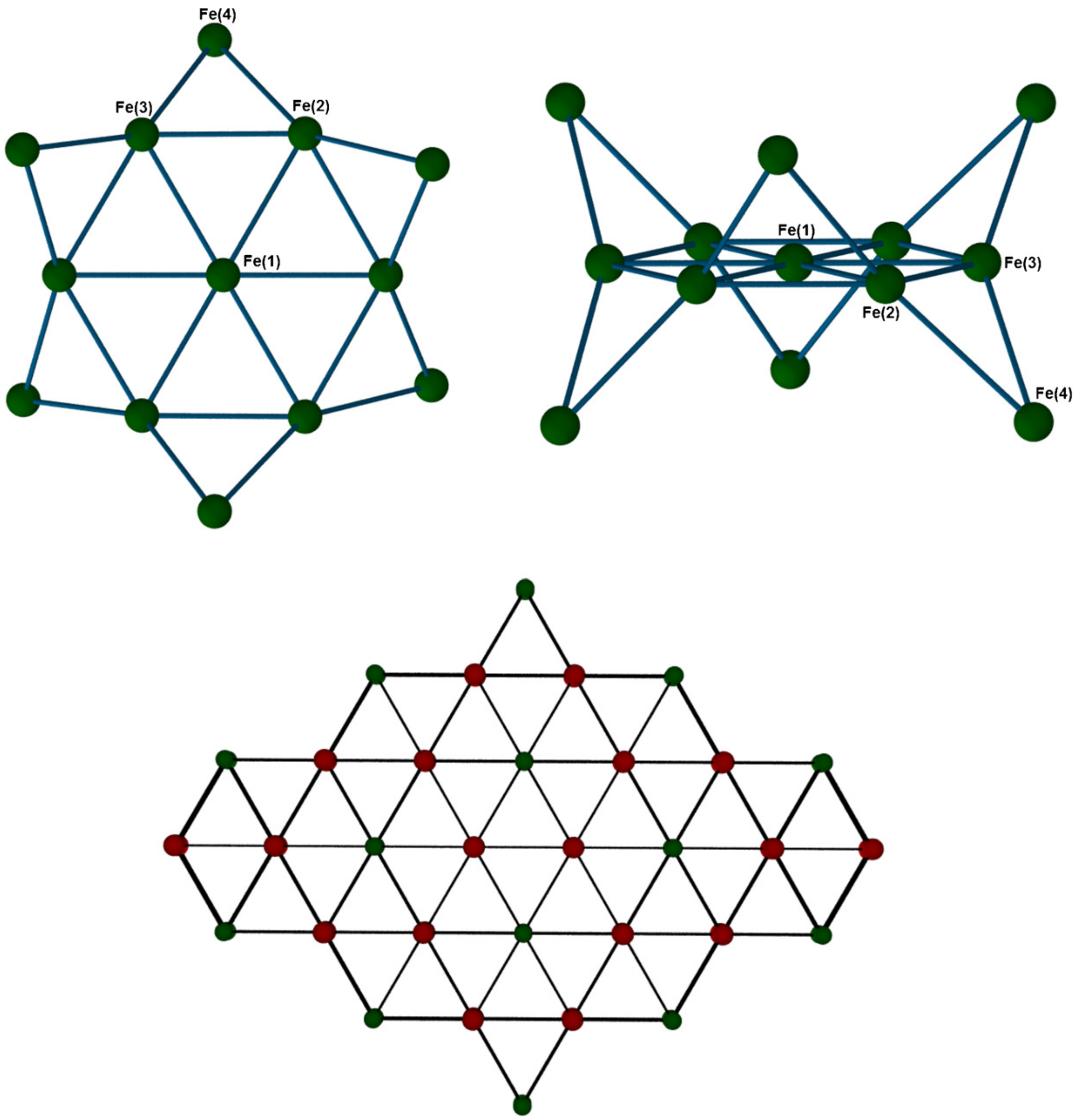

Fig. 16. The simplified version of both Fe_{13} clusters in **14** (upper) and the topological presentation of the SMOF KIT-100 (lower). Color code: (cluster A) green; (cluster B) red. (For interpretation of the references to color in this figure legend, the reader is referred to the web version of the article.)

3d–4f SMM. The molecular structure of **10** (Fig. 11) consists of a centrosymmetric $[Mn_5Dy_4]^{28+}$ core, held together by four $(\mu_3\text{-O})^{2-}$ and two $(\mu_4\text{-O})^{2-}$ ligands, and the oxygen atoms of two monodeprotonated $\eta^2:\eta^2:\eta^1:\mu_3$-diethanolamine and two doubly deprotonated $\eta^3:\eta^2:\eta^1:\mu_4$-diethanolamine ligands.

Simplifying the structure (Fig. 11 right), Mn(1) is converted to a 8-connected node with a vertex symbol $(3.3.3.3.3.3.3.3.3.3.3.3.4.4.4.4.4.4.4.4.4_2.4_2.5_2.5_2.5_2.5_2.5_4.5_4)$, while the remaining nodes are 4-connected and possess different vertex symbols with (3.3.3.4.3.4) for Mn(2) and Mn(3) and $(3.3.3.3.3.4_2)$ for Dy(1) and Dy(2). The cluster can thus be considered as three-nodal (4,8) with total symbol $(3^{12}.4^{10}.5^6)(3^4.4^2)_4(3^5.4)_4$.

2.11. *$[Mn_{14}O_2(OH)_4(ppo)_{18}(Hppo)_4(NO_3)_4(MeCN)_4]$*

Manganese polynuclear cluster chemistry has received tremendous attention owing to the anisotropy rising from Mn(III) with numerous of aesthetically pleasing structures being synthesized. An aesthetically pleasing mixed-valent tetradecanuclear $[Mn_{14}O_2(OH)_4(ppo)_{18}(Hppo)_4(NO_3)_4(MeCN)_4]$ **11** (Hppo = 3-phenyl-3-pyrazolin-5-one) Mn_{14} cage, containing two Mn(III) and 12 Mn(II) centers has been reported [23]. The core is based on Mn_7 fragments and two of these fragments are linked through two oxo bridges resulting in the Mn_{14} cage.

Simplifying the metal core (Fig. 12) of **11** Mn(4), Mn(5) and Mn(7) are 2-connected nodes with vertex symbol (3), Mn(1) is a 5-connected node with vertex symbol (3.3.3.3.3.3.4.4.4.4), Mn(2) and Mn(6) are also a 5-connected nodes with vertex symbols (3.3.3.3.3.4.4.4.5.5) and (3.3.3.3.4.4.4.4.5.5), respectively, and finally Mn(3) is a 6-connected node with vertex symbol (3.3.3.3.3.3.4.4.4.4.4.5.5.5.5). Overall the cluster can be described as five nodal (2,5,6) with total symbol $(3^4.4^4.5^2)_2(3^5.4^3.5^2)_2(3^6.4^4)_2(3^6.4^5.5^4)_2(3)_6$.

2.12. *$[Mn(II)_4Mn(III)_6O_4(N_3)_4(hmp)_{12}](X)_2$*

A mixed-valence manganese decanuclear cluster of formula $[Mn(II)_4Mn(III)_6O_4(N_3)_4(hmp)_{12}](X)_2$ **12** has an aesthetically pleasing structure of high (T) symmetry and is completely ferromagnetically coupled resulting in an $S = 22$ ground spin state supertetrahedron [24]. The cation $[Mn_{10}O_4(N_3)_4(hmp)_{12}]^{2+}$ consists of 10 Mn ions with a tetra-face-capped octahedral topology. The central octahedron comprises six Mn(III) ions, and the eight faces are bridged alternately by four azide ions and four μ_4-O^{2-} ions, with the latter also bridging to four external Mn(II) ions that thus cap four non-adjacent faces of the octahedron (Fig. 13).

Simplifying the core, the divalent Mn(1) defines a 3-connected node with vertex symbol (3.3.3), while the trivalent Mn(2) defines a 6-connected node with vertex symbol ($3.3.3.3.3.3.3.3.4.4.4.4.4_3.4_3.5_2$). Thus the cluster can be considered as binodal (3,6) with total symbol $(3^3)_4(3^8.4^6.5)_6$.

2.13. $[Mn(III)_{12}Mn(II)_7(\mu_4\text{-}O)_8(\mu_3,\eta^1\text{-}N_3)_8(HL)_{12}(MeCN)_6]Cl_2\cdot 10MeOH\cdot MeCN$

We were able to synthesize a Mn_{19} aggregate $[Mn(III)_{12}Mn(II)_7(\mu_4\text{-}O)_8(\mu_3,\eta^1\text{-}N_3)_8(HL)_{12}(MeCN)_6]Cl_2\cdot 10MeOH\cdot MeCN$ (**13**) which has a record $S = 83/2$ ground spin state [4]. The core of compound **13** (Fig. 14 upper) can be described as resulting from the fusion of two Mn_{10} corner-sharing supertetrahedra of the sort seen in compound **12** or else in terms of being based on two Mn_9 fragments linked through a common central Mn(II) center, Mn(1). This central manganese is unusual, being octacoordinated to six μ-O and two μ_4-O donor atoms. The topology of the metal core is relatively easy to describe in terms of regular polyhedra. For example, we can consider that each half of the molecule is derived from an almost perfect cube in which the vertices consist alternately of Mn(II) centers and central N atoms of the terminally coordinating μ_3-N_3 units. In this way it can readily be seen that the Mn(II) centers define a tetrahedron in each half of the molecule. At the center of each of the faces of each cube there is a Mn(III) center, thus defining an octahedron with the faces of the octahedron capped alternately by μ_3-N_3 and μ_4-O ligands, the latter of which is linked to the Mn(II) centers. This is in line with the idea that core structure of results from the formal fusion of two corner sharing Mn_{10} supertetrahedra of the type seen in compound **12**.

Simplifying the metal core of compound **13**, Mn(1) defines a 6-connected node with vertex symbol (3.3.3.3.3.3), while Mn(2) and Mn(3) are also 6-connected nodes with a vertex symbol ($3.3.3.3.3.3.3.3.4.4.4.4.4_3.4_3.5_2$) and finally Mn(4) represents a 3-connected node with vertex symbol (3.3.3). The Mn_{19} aggregate can be considered as 4-nodal (3,6) with total symbol $(3^3)_6(3^6)(3^8.4^6.5)_{12}$. In comparison with the supertetrahedron Mn_{10} **12** $(3^3)_4(3^8.4^6.5)_6$, thus the numerical presentation for both clusters also makes clear the topological similarities between **13** and **12**.

2.14. $[\{Fe_{13}(\mu_3\text{-}OH)_6(\mu_3\text{-}O)_6(Hntp)_8(H_2O)_6\}\{Fe_{13}(\mu_3\text{-}OH)_6(\mu_3\text{-}O)_6(Hntp)_8\}_2]\cdot 15NO_3\cdot 13H_2O$

In 2005, we published a hierarchical assembly of Fe_{13} oxygen-bridged clusters into a close-packed superstructure $[\{Fe_{13}(\mu_3\text{-}OH)_6(\mu_3\text{-}O)_6(Hntp)_8(H_2O)_6\}\{Fe_{13}(\mu_3\text{-}OH)_6(\mu_3\text{-}O)_6(Hntp)_8\}_2]\cdot 15NO_3\cdot 13H_2O$ (**14**) [25]. In this compound, two different kinds of Fe_{13} clusters can be found $[\{Fe_{13}(\mu_3\text{-}OH)_6(\mu_3\text{-}O)_6(Hntp)_8(H_2O)_6\}^{5+}$ (cluster A; Hntp = $HN(CH_2CH_2COO)_3$, Fig. 15 left) and $\{Fe_{13}(\mu_3\text{-}OH)_6(\mu_3\text{-}O)_6(Hntp)_8\}_2]^{5+}$ (cluster B, Fig. 15 right), which are extended into a 3D framework through carboxylate bridges forming the Super Metal Organic Framework (SMOF) KIT-100.

Adopting a similar simplification procedure, both clusters possess the same topology, therefore only one will be described. The central Fe(1) atom (cluster B, Fig. 15 right) is a 6-connected node connected to Fe(2) and Fe(3) atoms and the symbol is ($3.3.3.3.3.3.4.4.4.4.4.4.5_2.5_2.5_2$). Fe(2) and Fe(3) are 5-connected nodes with symbol (3.3.3.3.4.4.4.5.5.6), while the peripheral Fe(4) atoms are 2-connected nodes with symbol (3) (Fig. 16). Therefore, both clusters can be simplified to a 3-nodal (2,5,6) cluster with symbol $(3^4.4^3.5^2.6)_6(3^6.4^6.5^3)(3)_6$. The clusters are furthermore connected to one another through carboxylate bridges, forming a 3D structure. Every cluster can be considered as a 6-connected node, thus the topology of the final decorated compound can be classified as a pcu network close to the NaCl structure.

3. Conclusions

The improved synthetic strategies of inorganic chemistry have led to numerous polynuclear clusters. More and more complicated structures will be synthesized and reported. Our approach is to establish a new topological and numerical analysis which can easily be applied to both simple and complicated polynuclear clusters, with an emphasis on the numerical analysis of them. One important motivation for this approach is that the physicists, who can help in the description of the physical properties of systems, tend to prefer dealing with numbers rather than pictures. Finally, this approach makes it possible to create a library of topologically represented clusters, for example, which possess interesting magnetic properties, and useful conclusions might be arrived at after using this as a basis for a detailed study. A systematic categorization of such clusters has already been set up.

Acknowledgment

Financial support from the DFG Center for Functional Nanostructures is gratefully acknowledged.

References

[1] A. Müller, E. Beckmann, H. Bögge, M. Schmidtmann, A. Dress, Angew. Chem. Int. Ed. 41 (2002) 1162.
[2] C.E. Anson, A. Eichhöfer, I. Issac, D. Fenske, O. Fuhr, P. Sevillano, C. Persau, D. Stalke, J. Zhang, Angew. Chem. Int. Ed. 47 (2008) 1326.
[3] A.J. Tasiopoulos, A. Vinslava, W. Wernsdorfer, K.A. Abboud, G. Christou, Angew. Chem. Int. Ed. 43 (2004) 2117.
[4] A.M. Ako, I.J. Hewitt, V. Mereacre, R. Clérac, W. Wernsdorfer, C.E. Anson, A.K. Powell, Angew. Chem. Int. Ed. 45 (2006) 4926.
[5] A.K. Powell, S.L. Heath, D. Gatteschi, L. Pardi, R. Sessoli, G. Spina, F. Del Giallo, F. Pieralli, J. Am. Chem. Soc. 117 (1995) 2491.
[6] J. Han, D. Coucouvanis, J. Am. Chem. Soc. 123 (2001) 11304.
[7] B.F. Hoskins, R. Robson, J. Am. Chem. Soc. 112 (1990) 1546.
[8] B. Chen, M. Eddaoudi, T.M. Reineke, J.W. Kampf, M. O'Keeffe, O.M. Yaghi, J. Am. Chem. Soc. 122 (2000) 11599.
[9] G.E. Kostakis, L. Casella, N. Hadjiliadis, E. Monzani, N. Kourkoumelis, J.C. Plakatouras, Chem. Commun. (2005) 3859.
[10] M. O'Keeffe, M. Eddaoudi, H. Li, T. Reineke, O.M. Yaghi, J. Solid State Chem. 152 (2000) 3.
[11] J. Tang, I. Hewitt, N.T. Madhu, G. Chastanet, W. Wernsdorfer, C.E. Anson, C. Benelli, R. Sessoli, A.K. Powell, Angew. Chem. Int. Ed. 45 (2006) 1729.
[12] J. Luzon, K. Bernot, I.J. Hewitt, C.E. Anson, A.K. Powell, R. Sessoli, Phys. Rev. Lett. 100 (2008) 247205.
[13] L.F. Chibotaru, L. Ungur, A. Soncini, Angew. Chem. Int. Ed. 47 (2008) 4126.
[14] P. King, R. Clérac, W. Wernsdorfer, C.E. Anson, A.K. Powell, Dalton Trans. (2004) 2670.
[15] W. Schmitt, M. Murugesu, J.C. Goodwin, J.P. Hill, A. Mandel, R. Bhalla, C.E. Anson, S.L. Heath, A.K. Powell, Polyhedron 20 (2001) 1687.
[16] G. Wu, R. Clérac, W. Wernsdorfer, S. Qiu, C.E. Anson, I.J. Hewitt, A.K. Powell, Eur. J. Inorg. Chem. (2006) 1927.
[17] I.J. Hewitt, J.–K. Tang, N.T. Madhu, R. Clérac, G. Buth, C.E. Anson, A.K. Powell, Chem. Commun. (2006) 2650.
[18] A.M. Ako, O. Waldmann, V. Mereacre, F. Klöwer, I.J. Hewitt, C.E. Anson, H.U. Güdel, A.K. Powell, Inorg. Chem. 46 (2007) 756.
[19] Y. Li, W. Wernsdorfer, R. Clérac, I.J. Hewitt, C.E. Anson, A.K. Powell, Inorg. Chem. 45 (2006) 2376.
[20] A.M. Ako, V. Mereacre, R. Clérac, I.J. Hewitt, Y. Lan, C.E. Anson, A.K. Powell, Dalton Trans. (2007) 5245.
[21] V.M. Mereacre, A.M. Ako, R. Clérac, W. Wernsdorfer, G. Filoti, J. Bartolomé, C.E. Anson, A.K. Powell, J. Am. Chem. Soc. 129 (2007) 9248.

[22] V. Mereacre, A.M. Ako, R. Clérac, W. Wernsdorfer, I.J. Hewitt, C.E. Anson, A.K. Powell, Chem. Eur. J. 14 (2008) 3577.

[23] G. Aromí, A. Bell, S.J. Teat, A.G. Whittaker, R.E.P. Winpenny, Chem. Commun. (2002) 1896.

[24] T.C. Stamatatos, K.A. Abboud, W. Wernsdorfer, G. Christou, Polyhedron 26 (2007) 2042.

[25] M. Murugesu, R. Clérac, W. Wernsdorfer, C.E. Anson, A.K. Powell, Angew. Chem. Int. Ed. 44 (2005) 6678.